Journal of Alloys and Compounds 509 (2011) 6567–6570

Contents lists available at ScienceDirect

Journal of Alloys and Compounds

journal homepage: www.elsevier.com/locate/jallcom

Crystal growth and spectroscopic characterization of Yb-doped and Yb, Na-codoped PbF_2 laser crystals

Jigang Yin[a,b], Yin Hang[a,*], Xiaoming He[a], Lianhan Zhang[a], Chengchun Zhao[a,b], Pengchao Hu[a,b], Juan Gong[a,b]

[a] Key Laboratory of High Power Laser Materials, Shanghai Institute of Optics and Fine Mechanics, Chinese Academy of Sciences, Shanghai 201800, PR China
[b] Graduate School of Chinese Academy of Sciences, Beijing 100039, PR China

ARTICLE INFO

Article history:
Received 10 November 2010
Received in revised form 23 February 2011
Accepted 24 February 2011
Available online 3 March 2011

Keywords:
Bridgman
Laser crystal
Yb^{3+} doped

ABSTRACT

High-quality pure PbF_2, Yb:PbF_2 and Yb, Na:PbF_2 crystals are grown by the Bridgman method in a nonvacuum atmosphere. Room-temperature absorption, photoluminescence spectra, and fluorescence lifetimes belonging to the transitions between ground state $^2F_{7/2}$ and the excited state $^2F_{5/2}$ of Yb^{3+} ions in these crystals have been investigated. The influence of codoping with Na^+ ions on the spectra has been studied. Experimental results show that codoping Na^+ ions in different Na:Yb ratios can modulate the spectroscopy and photoluminescence properties of Yb^{3+} ions in a PbF_2 lattice in a large scope: the Na^+ ions codoping with Yb^{3+} as charge compensators can suppress the deoxidization of Yb^{3+} to Yb^{2+}, enhance the luminescence intensity and lengthen luminescence lifetime of Yb^{3+} ions.

1. Introduction

Yb^{3+} is the most promising ion that can be used in a non-Nd^{3+} laser in the near-IR spectral range of 1030 nm, which is roughly in the same range as Nd^{3+} emission wavelength, under laser diode pumping with a smaller quantum defect than in Nd^{3+}-doped crystals (10% instead of 25%). The Yb^{3+} ion has several advantages compared with Nd^{3+} due to its very simple energy level scheme, being composed of only two levels. This makes it possible to avoid up-conversion, excited state absorption and concentration quenching within a large concentration domain. Up to now, several oxides have been thoroughly investigated, and the spectroscopic properties of Yb^{3+}-doped host materials are leading to general methods of evaluation [1–7].

Recently, ytterbium-doped alkaline-earth fluorides (Yb:CaF_2, Yb:SrF_2, Yb:BaF_2) have attracted considerable interest for use in diode-pumped, femtosecond lasers and amplifiers [8,9]. These cubic crystalline structures have two main advantages: first, they have the possibility to grow them, either in the form of large-size transparent single crystals [10]; second, they have very good thermal properties [11], with thermal conductivities on the order of 10 W/m K for undoped crystals. It is obvious that in some Yb^{3+}-doped materials possessing higher thermal conductivity are favorable to exhibit the excellent laser performance of Yb^{3+} [12–15]. Hence, here we pay close attention to PbF_2 of cubic crystalline structures, which has higher thermal conductivity (28 W/m K) [16]. At low pressures, PbF_2 is found to exist in two structural phases, namely orthorhombic (α) and cubic (β). Although the cubic phase is the most stable in ambient conditions, the orthorhombic phase is stable at high pressure and low temperature. The cubic phase undergoes a phase transition at about 0.4 GPa to the orthorhombic phase and reverts back to the cubic phase at higher temperatures [17].

It is known that several of RE dopants, such as Sm, Eu, Ho and Yb, can be stabilized in the divalent state in alkaline earth halide lattices, besides the trivalent state, with which can coexist [18]. Some groups claimed that codoping with Li^+ or Na^+ ions in CaF_2 crystals drastically decrease the absorption intensity of the characteristic UV peaks of Yb^{2+} ions and the Pb-codoped Yb:CaF_2 crystals can promote the Yb^{3+}–Yb^{2+} conversion during the growth process [18,19]. However, Siebold and coworkers reported that it was possible to grow the crystals avoiding any trace of Yb^{2+} ions without involving Na^+ ions. It is just a question of growth atmosphere [20]. In view of the reasons mentioned above, the Yb-doped and Yb, Na-codoped PbF_2 single crystals were grown, the spectroscopic properties of Yb ions and the effect of Na^+ ions in the single crystals were investigated.

2. Experimental

The pure PbF_2, YbF_3-doped and YbF_3, NaF-codoped PbF_2 crystals were grown in our crystal research laboratory using the conventional technique modified Bridgman method under non-vacuum conditions. The orthorhombic PbF_2 (99.99%), NaF

* Corresponding author.
E-mail address: yhang@siom.cn.com (Y. Hang).

0925-8388/$ – see front matter © 2011 Published by Elsevier B.V.
doi:10.1016/j.jallcom.2011.02.140

(99.99%) and YbF_3 (99.99%) powders have been used as starting material for the growth process. The raw material was heated again at 120–180 °C for 4–6 h in dried CF_4 atmosphere. The platinum crucible used in crystal growth was 30–40 mm in diameter and 150–180 mm long with conical bottom. After the dehydration treatment had finished, the raw material was filled in the crucible. To avoid the oxidation and volatilization of the melt, the assembled crucible was sealed immediately. However, there was always a volume of air that remained in the crucible when it was sealed. So a chemical (rubber or carbon powder) that can scavenge oxygen impurities, such as O^{2-} and OH^-, and does not cause any harmful effects on the crystal properties and growth equipment, was added to the top of the raw material so as to exhaust the air sealed in the crucible during the crystal growth.

The resistively heated vertical Bridgman furnace used in the crystal growth and the temperature of the furnace was controlled by a computer during the entire growing process. According to the temperature distribution, the furnace chamber consists of three zones, i.e., the high-temperature zone, the gradient zone, and the low-temperature zone. The melt was homogenized in the crucibles in the high-temperature zone, while the grown crystal could be annealed in the low-temperature zone. The solid-liquid interface was located in the gradient zone. The high-temperature zone was controlled at 960 °C. To detect the axial temperature along the crucible and the temperature gradient at solid-liquid interface during the entire growing process, it was fitted with two Pt–Pt/Rh 10% thermocouples, as shown in Fig. 1(a). The temperature curves of the entire growing process recorded by computer are given in Fig. 1(b). The temperature gradient across the solid-liquid interface was around 30 °C/cm. The growth process was driven by lowering the crucible at a rate of 0.5–0.8 mm/h. After the growth had finished, the furnace was cooled to room temperature at the rate of 30–40 °C/h.

X-ray diffraction analysis of the grown crystal was performed with a Rigaku D/max 2550 V diffractometer, using monochromatic Cu Kα radiation with a working voltage of 40 kV and current of 100 mA. The concentration of Yb was measured by inductively coupled plasma atomic emission spectrometry analysis. The absorption spectra of the grown crystals were recorded by a Jasco V-570 UV/VIS/NIR spectrophotometer. The luminescence spectra of Yb^{2+} and Yb^{3+} in Yb-, and Yb, Na-doped PbF_2 crystals were obtained with Nikon G250 spectrophotometer and Triax550 spectrofluorimeter. These samples with uniform dimensions were measured under the same conditions to compare the luminescence intensity and the emission lifetimes. All the measurements were taken at room temperature.

3. Results and discussion

The as-grown crystals are shown in Fig. 2(a). Cracks, bubbles and inclusions were not observed. Fig. 2(b) presents the X-ray diffraction pattern of the crystals. No other phase is found in the sample and the XRD patterns of the doped crystal matched very well with that of the undoped sample, which means the doping did not change the crystal structure. The ionic radiuses of Yb and Na ions are smaller than of the Pb ions. The substitution of Yb and Na ions for Pb ions induces lattice aberrance, which resulted in a slight shift of peak position and crystal lattice constant of the doped decreased in compared with that of the pure crystals, as shown in Table 1, and the change will be evident with the more doping concentration.

The absorption spectra of Yb-, and Yb, Na-doped PbF_2 crystals are obtained and reveal the existence of both $Yb^{2+}$and Yb^{3+} ions, with characteristic bands in UV region for Yb^{2+} ions (displayed in Fig. 1 of Ref. [21]), respectively, in near-IR for Yb^{3+} ions (Fig. 3(a)). The absorption spectra of Yb^{3+} are characterized by a very broad band in near-IR spectral domain, corresponding to the electronic transition from the $^2F_{7/2}$ ground state to the $^2F_{5/2}$ excited states of the Yb^{3+} ions [22]. The two absorption bands peaks at 338 nm (A_1) and 367 nm (A_2) in Fig. 1 of Ref. [21], which may originate from the Yb^{2+} ion accompanied by an impurity or a lattice vacancy and the $4f^{14}$–$4f^{13}5d$ transitions of isolated Yb^{2+} ions (O_h site), respectively [22,23]. For thorough testify the existing of Yb^{2+} ions and the impact of Na ions, the room temperature emission spectrum of Yb-, and Yb, Na-doped PbF_2 crystals excited with the 338 nm wavelength are shown in Fig. 3(b). The result showed that there exists a broad emission band originating from the Yb^{2+} ion which ranges from 350 nm to 500 nm, centered at 400 nm, also reported in [18,19]. The emission spectra of these crystals reveal the same phenomenon as the absorption spectra displayed in Fig. 1 of Ref. [21]: the Na^+-codoped can reduce the content of the Yb^{2+} ion in the crystals.

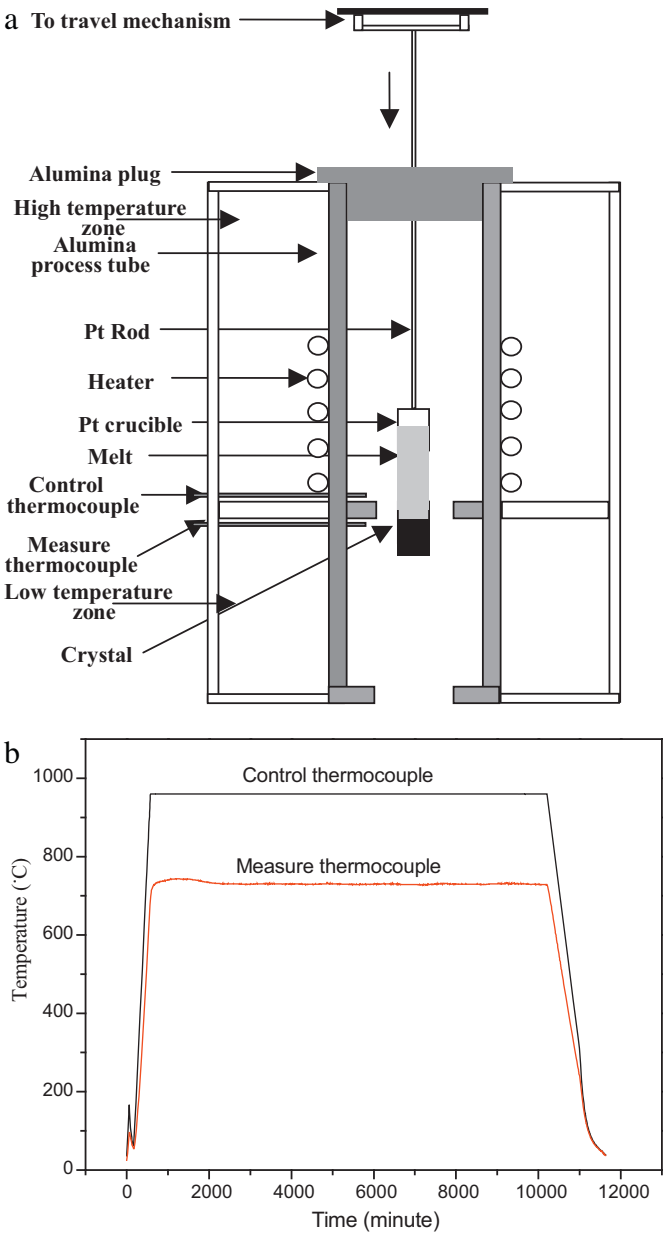

Fig. 1. (a) Scheme of the vertical Bridgman furnace. (b) The temperature curve at solid-liquid interface during the entire growing process. (I) PbF_2, (II) Yb (2%):PbF_2 and (III) Yb (2%), Na (2%):PbF_2.

The β-PbF_2 structure consists of a simple cubic lattice of fluorine ions in which every other body center position is occupied by a Pb^{2+} ion. The Yb^{3+} ions usually occupy a cation substitutional position, but charge compensation is required to maintain the electrical neutrality of the system. The extra positive charge is compensated by an interstitial fluorine ion (F_i^-). Several cases are possible, according to the position of the interstitial F_i^-: first, the interstitial F_i^- is situated in another unit cell than the one containing the Yb ion, preserving the cubic local symmetry (O_h) of the Yb ion. Second, the interstitial fluoride is situated in the same unit cell as the Yb ion, inducing a distortion from the cubic symmetry. Hence, the Yb ion symmetry centers are either tetragonal (C_{4v}) if the interstitial F_i^- is situated in the [1 0 0] direction, or trigonal (C_{3v}) if it is situated in the [1 1 1] direction [24]. After introducing intended Na^+ ions in the crystal, the sites of Yb^{3+} are predominantly C_{2v} in which Na^+ substitutes one of the eight nearest neighbor Pb^{2+} ions along any [1 1 0] direction and form a charge-neutralized Yb^{3+}–Na^+ ion

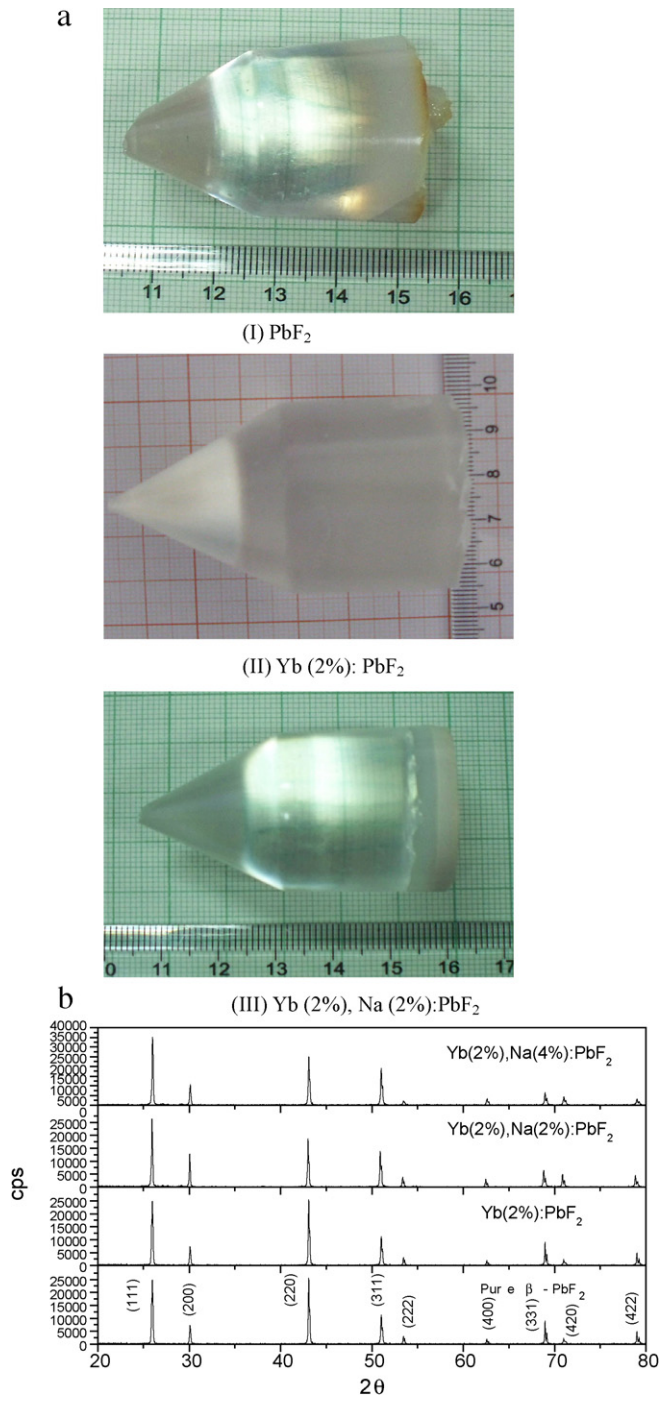

Fig. 2. (a) Photograph of lead fluoride crystals: (I) PbF_2, (II) Yb:PbF_2 and (III) Yb, Na:PbF_2. (b) X-ray diffraction pattern of the grown crystal

pair and do not require charge compensation. This phenomenon should be same as the results of the Yb, Na:CaF_2 crystal [25]. Hence, compared to the interstitial fluoride anions, the Na^+ ions are more effective to compensate the valence mismatch in Yb:PbF_2 crystal and suppresses the formation of Yb^{2+} ions.

Table 1
The parameters of Yb-, and Yb, Na-doped PbF_2.

Sample	a (Å)	V (Å^3)
PbF_2	5.9425 ± 0.00002	209.81
Yb (2%):PbF_2	5.9046 ± 0.00002	209.23
Yb (2%), Na (2%):PbF_2	5.8898 ± 0.00002	208.21
Yb (2%), Na (4%):PbF_2	5.87963 ± 0.00002	207.58

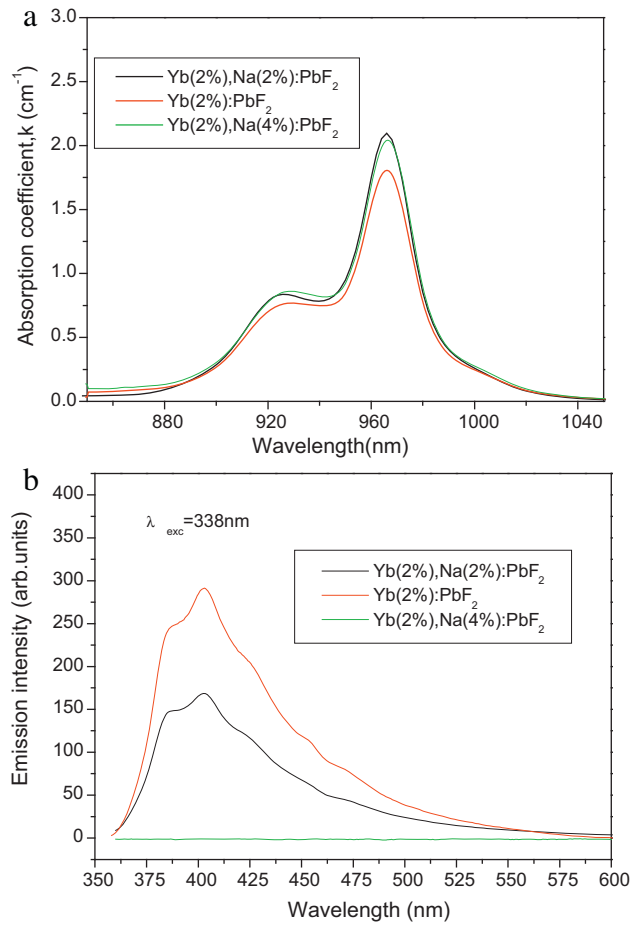

Fig. 3. (a) Absorption spectra of Yb-, and Yb, Na-doped PbF_2 in near-IR for Yb^{3+} ions. (b) Emission spectra of Yb-, and Yb, Na-doped PbF_2 for Yb^{2+} ions.

The luminescence spectra and the lifetimes of the emission intensity at 1010 nm of Yb^{3+} in Yb-, and Yb, Na-doped PbF_2 crystals under 940-nm laser diode excitation were obtained, as shown in Figs. 4 and 5. We can see that the Na^+ ions introduced as charge compensator enhances the emission intensity and broadens the emission bands. The change is more significant increasing with the Na:Yb ratio from 1:1 to 2:1 further. The infrared Yb^{3+} ($^2F_{5/2}$) fluorescence decays exponentially with the lifetimes equal to 2.30, 2.44, and 2.67 ms in these crystals, respectively. The emission lifetime of Yb^{3+} in crystal is increased by the addition of Na^+ and by

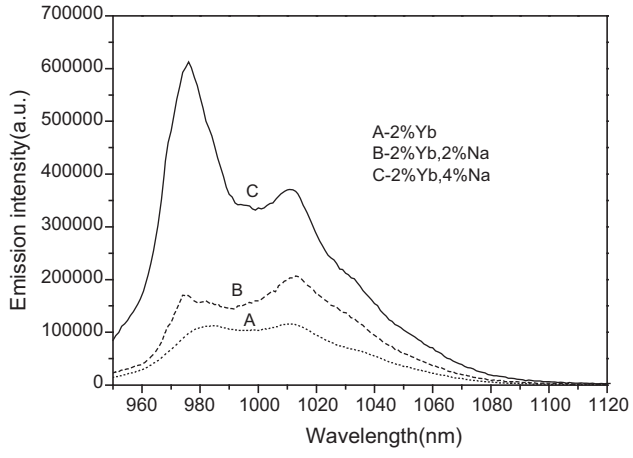

Fig. 4. Room-temperature fluorescence spectra of the crystals pumped at 940 nm.

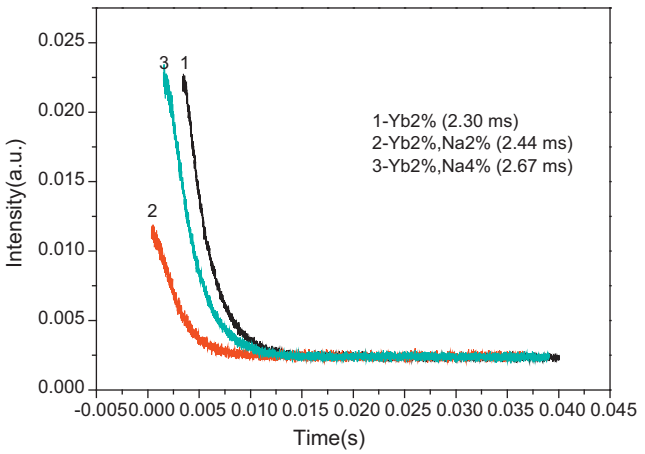

Fig. 5. Room-temperature fluorescence decay curves of the grown crystals at 1010 nm.

Table 2
The laser parameters of Yb-, and Yb, Na-doped PbF_2.

Sample	FWHM of emission band	Wavelength (nm)	Emission cross section (10^{-20} cm^2)	Radiative lifetime (ms)
Yb (2%):PbF_2	58	1012	0.40	2.30
Yb (2%), Na (2%):PbF_2	58	1012	0.41	2.44
Yb (2%), Na (4%):PbF_2	53	1012	0.28	2.67

raising the proportion of Na:Yb. It is substantiated that Yb^{3+} form cluster structures involving at least Yb^{3+}–Yb^{3+} ions pairs in adjacent cubes in Yb (2%):PbF_2 crystal [24]. Similar to the Yb^{3+} in CaF_2 crystal, fluorescence quenching will appear through cooperative luminescence between Yb^{3+}–Yb^{3+} pairs in Yb:PbF_2 crystal [4]. Moreover, the existence of Yb^{2+} can induce fluorescence quenching of the Yb^{3+} emission. The cooperative process among the excited Yb^{3+} ions and one nonexcited Yb^{2+} ion, where the simultaneous de-excitation of the Yb^{3+} ions results in a nonradiative energy transfer to the Yb^{2+}. Na^+ introduced as a charge compensator replaces Pb^{2+} in the nearest neighbor of Yb^{3+} and forms a charge-neutralized Yb^{3+}–Na^+ ion pair, which suppresses the formation of Yb^{2+} ions and prevents Yb^{3+} ions from clustering. Hence, the luminescence quantum efficiency of Yb^{3+} ions in a PbF_2 lattice was greatly improved. The stronger luminescence intensity and the longer luminescence lifetime are obtained as a result of high quantum efficiency. The laser parameters of Yb^{3+} ions in Yb-, and Yb, Na-doped PbF_2 crystals are presented in Table 2, which can be modulated through introducing Na^+ as a charge compensator with different Na:Yb ratios.

4. Conclusions

Bridgman-grown Yb:PbF_2 and Yb, Na:PbF_2 crystals have been investigated for their growth, the spectroscopic properties of Yb ions and the effect of Na^+ ion in the single crystals. The absorption spectra, photoluminescence properties, and fluorescence lifetime of Yb^{3+} ions can be modulated by introducing Na^+ as a charge compensator with different Na:Yb ratios. These results can reveal for us to develop Yb^{3+}-doped diode-pumped solid-state lasers with different laser performance for various applications.

References

[1] G. Boulon, A. Brenier, L. Laversenne, Y. Guyot, C. Goutaudier, M.T. Cohen-Adad, G. Metrat, N. Muhlstein, J. Alloys Compd. 341 (2002) 2.
[2] S.S. Cheng, X.D. Xu, D.Z. Li, D.H. Zhou, F. Wu, Z.W. Zhao, J. Xu, J. Alloys Compd. 506 (2010) 513.
[3] M. Koyama, T. Hirose, M. Okida, K. Miyamoto, T. Omatsu, Opt. Exp. 19 (2011) 994.
[4] I. Masahiko, G. Christelle, G. Yannick, L. Kheirreddine, F. Tsuguo, B. Georges, J. Phys. Condens. Matter 16 (2004) 1501–1521.
[5] F. Balembois, M. Castaing, P. Georges, T. Georges, J. Opt. Soc. Am. B 28 (2011) 115.
[6] O. Khasanov, V. Osipov, E. Dvilis, A. Kachaev, A. Khasanov, V. Shitov, J. Alloys Compd. (2010) 140, doi:10.1016/j.jallcom.2011.01.
[7] A. Wojciechowski, M. Swirkowicz, A. Karas, L.R. Jaroszewicz, A. Majchrowski, E. Gondek, K. Ozga, I.V. Kityk, J. Alloys Compd. 504 (2010) 197.
[8] A. Lucca, G. Debourg, M. Jacquemet, F. Druon, F. Balembois, P. Georges, P. Camy, J. Doualan, R. Moncorgé, Opt. Lett. 29 (2004) 2767.
[9] P. Camy, J. Doualan, A. Benayad, M. von Edlinger, V. Ménard, R. Moncorgé, Appl. Phys. B 89 (2007) 539.
[10] S.E. Hatch, W.F. Parsons, R. Weagley, J. Appl. Phys. Lett. 5 (1964) 153.
[11] R. Gaumé, B. Viana, D. Vivien, J.P. Roger, D. Fournier, Appl. Phys. Lett. 83 (2003) 1355–1357.
[12] W.F. Krupke, IEEE J. Sel. Top. Quantum Electron. 6 (2000) 1287–1296.
[13] C. Kränkel, D. Fagundes-Peters, S.T. Fredrich, J. Johannsen, M. Mond, G. Huber, M. Bernhagen, R. Uecker, Appl. Phys. B 79 (2004) 543–546.
[14] P. Dekker, J.M. Dawes, J.A. Piper, Y.G. Liu, J.Y. Wang, Opt. Commun. 195 (2001) 431–436.
[15] E. Montoya, J.A. Sanz-García, J. Capmany, L.E. Bausá, A. Diening, T. Kellner, G. Huber, J. Appl. Phys. 87 (2000) 4056–4062.
[16] W.J. Tropf, M.F. Thomas, T.J. Harris, Handbook of Optics, vol. 2, McGraw-Hill, New York, 1995, pp. 33–51.
[17] J. Huitian, O. Roberto, A.B. Miguel, P. Ravindra, J. Phys. Condens. Matter 16 (2004) 3081–3088.
[18] N. Irina, L. Liliana, E. Monica, E. Ionut, J. Cryst. Growth 310 (2008) 2026–2032.
[19] N. Irina, S. Marius, P. Andreea, J. Cryst. Growth 310 (2008) 1470–1475.
[20] M. Siebold, S. Bock, U. Schramm, B. Xu, J.L. Doualan, P. Camy, R. Moncorgé, Appl. Phys. B 97 (2009) 327–338.
[21] J.G. Yin, Y. Hang, X.Y. Liang, X.M. He, J.F. Li, L.H. Zhang, C.C. Zhao, P.C. Hu, Opt. Lett. 35 (2010) 3435.
[22] M. Itto, C. Goutaudier, Y. Guyot, K. Lebbou, T. Fukuda, G. Boulon, J. Phys. Condens. Matter 16 (2004) 1501.
[23] S.M. Kaczmarek, T. Tsuboi, M. Ito, G. Boulon, G. Leniec, J. Phys. Condens. Mater 17 (2005) 3771–3786.
[24] G. Dantelle, M. Mortier, Ph. Goldner, D. Vivien, J. Phys. Condens. Matter 18 (2006) 7905–7922.
[25] J. Kirton, S.D. Mclaughlan, Phys. Rev. 155 (1967) 279–284.